HHS Public Access

Author manuscript

Leukemia. Author manuscript; available in PMC 2022 August 01.

Published in final edited form as:

Leukemia. 2022 February ; 36(2): 492–506. doi:10.1038/s41375-021-01423-x.

Spred1 deficit promotes treatment resistance and transformation of chronic phase CML

Junjing Qiao[1,2,3,#], **Chen Liang**[2,4,#], **Dandan Zhao**[2,#], **Le Xuan Truong Nguyen**[2], **Fang Chen**[2], **Shanshan Suo**[2,5], **Dinh Hoa Hoang**[2], **Francesca Pellicano**[6], **Ivan Rodriguez Rodriguez**[2], **Yasmin Elhajmoussa**[2], **Lucy Ghoda**[2], **Akihiko Yoshimura**[7], **Anthony S Stein**[2], **Haris Ali**[2], **Paul Koller**[2], **Danilo Perrotti**[8], **Mhairi Copland**[6], **Anjia Han**[1,*], **Bin Zhang**[2,*], **Guido Marcucci**[2,*]

[1]Department of Pathology, the First Affiliated Hospital, Sun Yat-Sen University, Guangzhou, Guangdong, PR China

[2]Department of Hematological Malignancies Translational Science, Gehr Family Center for Leukemia Research, City of Hope Medical Center and Beckman Research Institute, Duarte, CA, USA

[3]Phase I Clinical Research Center, The Affiliated Cancer Hospital of Zhengzhou University & Henan Cancer Hospital, Zhengzhou, Henan, PR China.

[4]State Key Laboratory of Experimental Hematology, National Clinical Research Center for Blood Diseases, Institute of Hematology & Blood Diseases Hospital, Chinese Academy of Medical Sciences & Peking Union Medical College, Tianjin, PR China

[5]Department of Hematology, the First Affiliated Hospital, College of Medicine, Zhejiang University, Hangzhou, Zhejiang, PR China

[6]Paul O' Gorman Leukemia Research Centre, College of Medical, Veterinary and Life Sciences, Institute of Cancer Sciences, University of Glasgow, Glasgow, UK

[7]Department of Microbiology and Immunology, Keio University School of Medicine, Tokyo, Japan

[8]University of Maryland, Baltimore, MD, USA.

[*]Correspondence should be addressed to: Bin Zhang, City of Hope Medical Center, 1500 E Duarte Road, Duarte, CA 91010, USA. Phone: 626-359-8111; Fax: 626-301-8973. bzhang@coh.org or Anjia Han, Department of Pathology, the First Affiliated Hospital, Sun Yat-Sen University, Guangzhou, Guangdong, PR China. Phone: 86-20-87332235; Fax: 86-20-87332235. hananjia@mail.sysu.edu.cn. or Guido Marcucci, City of Hope Medical Center, 1500 E Duarte Road, Duarte, CA 91010, USA. Phone: 626-218-2705; Fax: 626-301-8973. gmarcucci@coh.org.

[#]contributed equally.

Authors' contributions

JQ designed and conducted experiments, analyzed data, wrote the manuscript; CL, DZ and L.X.T.N designed and conducted experiments and analyzed data; FC, SS, DHH, FP, IRR and YE conducted experiments; LG provided patient samples; AY provided Spred1 KO and Spred1$^{flox/flox}$ mice and reviewed the manuscript; AS, HA, PK, and DP reviewed data and the manuscript; MC and AH reviewed data and the manuscript and provided administrative support; BZ and GM designed experiments, analyzed data, wrote manuscript and provided administrative support.

Conflict of interest

The authors declare that they have no conflict of interest.

Ethics declarations

Patient sample acquisition was approved by the Institutional Review Boards (IRB) at the COHNMC, in accordance with an assurance filed with and approved by the Department of Health and Human Services and met all requirements of the Declaration of Helsinki. CML patients were consented on the IRB #18067 protocol.

Abstract

Spred1 is highly expressed in normal hematopoietic stem cells (HSCs). Lack of Spred1 function has been associated with aberrant hematopoiesis and acute leukemias. In chronic myelogenous leukemia (CML), Spred1 is reduced in patients with accelerated phase (AP) or blast crisis (BC) CML, thereby suggesting that deficit of this protein may contribute to disease transformation. In fact, Spred1 knockout (KO) in SCLtTA/BCR-ABL CML mice either globally, or restricted to hematopoietic cells (i.e., HSCs) or to endothelial cells (ECs), led to transformation of chronic phase (CP) CML into AP/BC CML. Upon BCR-ABL induction, all three Spred1 KO CML models showed AP/BC features. However, compared with global Spred1 KO, the AP/BC phenotypes of HSC-Spred1 KO and EC-Spred1 KO CML models were attenuated suggesting a concurrent contribution of Spred1 deficit in multiple compartments of the leukemic bone marrow niche to the CML transformation. Spred1 KO, regardless if occurred in HSCs or in ECs, increased miR-126 in LSKs ($Lin^{-}Sca\text{-}1^{+}c\text{-}Kit^{+}$, enriched in leukemic stem cells (LSCs)], resulting in expansion of LSCs, likely through hyperactivation of the MAP/ERK pathway that augmented Bcl-2 expression and stability. This ultimately led to enhancement of Bcl-2-dependent oxidative phosphorylation that supported homeostasis, survival and activity of LSCs and drove AP/BC transformation.

Graphical Abstract

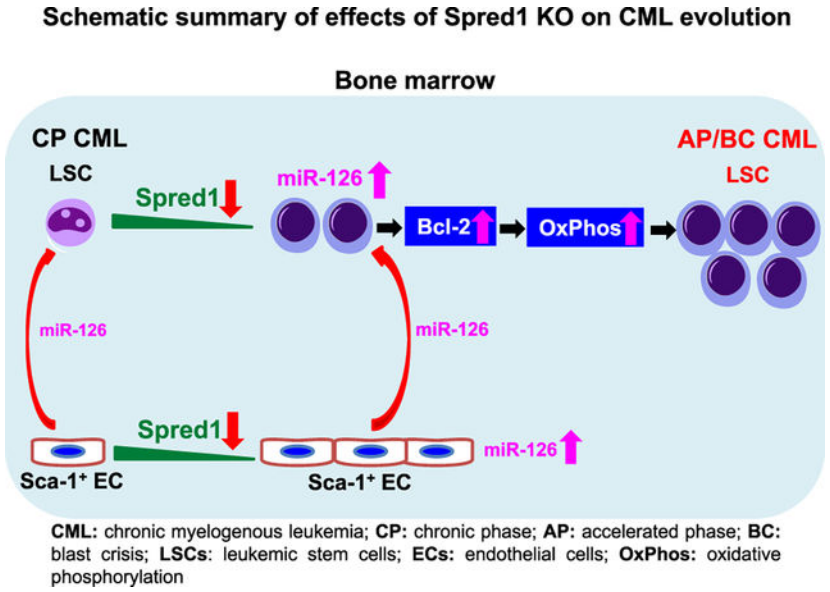

Introduction

Chronic myeloid leukemia (CML) is a myeloproliferative disorder characterized by the Philadelphia (Ph) chromosome derived from translocation of chromosomes 9q34 and 22q11[1]. The translocation creates a fusion oncogene, BCR–ABL1, that encodes a chimeric tyrosine kinase (TK) protein capable of transforming pluripotent hematopoietic stem cells (HSCs) into leukemic stem cells (LSCs), and therefore of initiating and maintaining leukemogenesis. Even though CML patients respond well to tyrosine kinase inhibitors (TKIs) in the chronic phase (CP) of the disease, the majority of them are committed to a life-

long treatment since LSCs may persist and lead to either disease relapse or progression to an accelerated phase (AP) and eventually to a blast crisis (BC)[2]. Unfortunately, once the disease has progressed to AP/BC, allogeneic stem cell transplantation is the only potential curative approach, but this procedure carries a relatively high risk of treatment-related toxicity and death, and disease relapse remains possible[2, 3]. Thus, understanding the molecular mechanisms of disease evolution and eradicating LSCs with novel, safer and more effective approaches are unmet needs for patients with CML.

In our quest for novel therapeutic targets that would allow us to eliminate CML LSCs, we recently focused on SPRED1 (Sprouty-related protein with EVH1 Domain 1), a member of the SPRED protein family that also comprises SPRED2 and SPRED3[4]. SPRED1 is a downstream substrate for both TKs (i.e., FLT3, KIT) and phosphatases (i.e., SHP2, SHIP1) that respectively enhance and attenuate its signaling functions[5, 6], and also is a recognized upstream inhibitor of small GTPases including RAS, ROCK, and RAN[7, 8].

Germline loss-of-function mutations of *SPRED1* cause Legius syndrome, one of the recognized "RASopathies", a group of RAS-MAPK pathway-related genetic syndromes[9]. While Legius syndrome has not been previously associated with leukemia, more recently, acquired loss-of-function mutations of *SPRED1* have been found in pediatric AML patients[10, 11]. Furthermore, lower *SPRED1* expression has been observed in FLT3-ITD+ AML[12] and predicted for poor outcome[10, 11, 13]. Of note, *Spred1* knockout (KO) (*Spred1*$^{-/-}$) mice do not develop leukemia[14], suggesting that other genetic or microenvironmental co-factors are necessary to elicit a malignant phenotype. To this end, *Spred1* KO mice fed a high-fat diet (HFD) develop a myeloproliferative disorder (MPD), possibly due to a HFD-induced RAS-MAPK hyperactivation by gut microbiota dysbiosis[14].

Of note, SPRED1 is also a regulator of miR-126 that we proved to be relevant to LSC homeostasis and self-renewal in CML[15, 16]. Herein, we report on the leukemogenic role of Spred1 deficit in CML. We showed that Spred1 KO, either globally or restricted to the hematopoietic or vascular compartment of the leukemic bone marrow (BM) niche, induced TKI resistance and disease transformation from CP to AP/BC CML via miR-126 overexpression in LSCs. This contributed to the enhancement of oxidative metabolism and in turn expansion and hyperactivity of LSCs that drove disease transformation in normally fed CML mice (Summary Figure).

Materials and methods

An extended description of the methods is in the Supplementary information.

Human samples

CP and BC CML samples were obtained from patients who had not received TKI treatment at the City of Hope National Medical Center (COHNMC). All CML samples used in this study are P210 BCR–ABL positive, as confirmed by FISH analysis and qPCR. Mononuclear cells (MNCs) were isolated using Ficoll separation. Sample acquisition was approved by the Institutional Review Boards (IRB) at the COHNMC, in accordance with an assurance filed with and approved by the Department of Health and Human Services and met all

requirements of the Declaration of Helsinki. Patients with CML were consented on the IRB #18067 protocol.

Animal studies

SCLtTA/BCR-ABL transgenic mice [C57BL/6(B6)-Ly5.2][17, 18] were maintained on tetracycline (tet)-containing water at 0.5 g/liter. Withdrawal of tet results in expression of BCR–ABL and generation of a CML-like disease in these mice[17, 18]. Spred1 KO CML (i.e., Spred1$^{-/-}$SCLtTA/BCR-ABL, B6-Ly5.2) mice were generated by crossing Spred1$^{-/-}$ mice[19] with SCLtTA/BCR-ABL mice. SCLtTA/BCR-ABL mice in B6-Ly5.1/Ly5.2 background were generated by breeding B6-Ly5.2 SCLtTA/BCR-ABL with B6-Ly5.1 mouse and used as donors. *Spred1$^{flox(f)/f}$* (B6-Ly5.2)[19, 20] mice were crossed with Mx1-Cre-positive (+) (B6-Ly5.2; Jax lab, #2527) and Tie2-Cre+ (B6-Ly5.2; Jax lab, #8863) mice respectively to generate Spred1$^{f/f}$Mx1-Cre+ (Spred1 KO in HSCs, hereafter called Spred1$^{HSC\Delta/\Delta}$) and Spred1$^{f/f}$Tie2-Cre+ [Spred1 KO in endothelial cells (ECs), hereafter called Spred1$^{EC\Delta/\Delta}$] mice. Spred1$^{HSC\Delta/\Delta}$ and Spred1$^{EC\Delta/\Delta}$ mice were further crossed with SCLtTA/BCR–ABL mice to obtain Spred1$^{HSC\Delta/\Delta}$SCLtTA/BCR-ABL (HSC-Spred1 KO) and Spred1$^{EC\Delta/\Delta}$SCLtTA/BCR-ABL (EC-Spred1 KO) mice. The genotyping of the above mice was performed by Transnetyx. To induce Cre recombinase, *Spred1$^{f/f}$Mx1-Cre* and *SCLtTA/BCR-ABL/Spred1$^{f/f}$/Mx1-Cre* mice were treated with 7 doses (250 μg/dose; every 2 days) of polyinosinic:polycytidylic acid [poly(I:C)]. BCR-ABL expression was induced for two to four weeks by tet withdrawal as indicated, then BM cells (from both tibias and femurs) were collected for experiments. Eight weeks old B6-Ly5.1 (from Charles River) mice were irradiated at 6Gy within 24 hrs before transplantation and used as recipients to allow tracking of B6-Ly5.2 or Ly5.1/5.2 donor cells. The number of mice for each study group was chosen based on the expected endpoint variation (i.e., engraftment rate and latency period of leukemia) and on the availability of mice from different strains. Mice of the same gender and age were randomly divided into groups. Investigators were blinded to mouse genotype while performing treatment or monitoring for engraftment or survival. Mouse care and experimental procedures were performed in accordance with federal guidelines and protocols and were approved by the Institutional Animal Care and Use Committee at City of Hope.

Flow cytometry analyses

Human CD34^{+} cells were selected using the indirect CD34 microbead kit (Miltenyi Biotec, San Diego, CA) and CD34^{+}CD38^{-} cells were sorted after staining with human antibodies against CD34 and CD38 (Supplementary Table 1) or selected using CD34+CD38- cell isolation kit (Miltenyi Biotec, San Diego, CA) according to the manufacturer's protocol. Mouse cells were obtained from peripheral blood (PB), BM (from both tibias and femurs), and/or spleen. To analyze or sort stem and progenitor cells in BM and spleen, we often selected c-kit^{+} cells using anti-mouse CD117 microbeads or Lineage^{-} (Lin^{-}) cells using lineage depletion microbeads (both from Miltenyi Biotec, San Diego, CA) first and then stained the cells with mouse antibodies (Supplementary Table 1) for further analysis or sorting for HSCs (Lin^{-}Sca-1^{+}c-Kit^{+}, LSK) or long-term (LT) HSCs (CD150^{+}CD48^{-} LSK). BM ECs were also isolated (see Supplementary methods for details) and then stained with antibodies (Supplementary Table 1). ECs were identified as CD45^{-}Ter119^{-}CD31^{+}. Sca-1^{high}

and Sca-1^{low} EC subfractions in BM were analyzed or sorted for *in vitro* experiments. To determine the frequency of quiescent LT-HSCs, cell cycle was analyzed by Ki-67-Alexa Fluor 647 (B56, BD) and DAPI (BD) labeling based on the manufacturer's protocol. All analyses were performed on a Fortessa x20 flow cytometer (BD Biosciences) and sorting was performed on Aria Fusion instrument (BD Biosciences) and data were analyzed by BD FACSDiva or FlowJo software.

Immunofluorescent staining and 3D confocal imaging of long bones

Long bones (tibias or femurs) from the mice were processed, sectioned and imaged as described previously[21] with ad-hoc modifications (see supplementary methods for details).

In vivo treatment of mice

To evaluate the impact of HSC-Spred1 KO on leukemia evolution, BM cells obtained from poly(I:C)-treated and BCR-ABL-induced (three weeks after tet withdrawal) *Spred1*$^{HSCwild\text{-}type(wt)/wt}$*SCLtTA/BCR-ABL* and *Spred1*$^{HSC\Delta/\Delta}$*SCLtTA/BCR-ABL* mice (B6-Ly5.2) were transplanted by tail vein injection (10^6 cells/mouse) into irradiated (6Gy) normal wt recipient mice (B6-Ly5.1). Two weeks after transplantation, these mice were divided into four groups and treated with nilotinib (NIL, 50 mg/kg, daily by oral gavage) or vehicle (HSC wt+vehicle, HSC wt+NIL, HSC KO+vehicle, HSC KO+NIL) for three weeks. To evaluate the impact of EC-Spred1 KO on leukemia evolution, after two weeks of BCR-ABL induction by tet withdrawal, *Spred1*$^{ECwt/wt}$*SCLtTA/BCR-ABL* and *Spred1*$^{EC\Delta/\Delta}$*SCLtTA/BCR-ABL* mice were treated with NIL (50 mg/kg, daily by oral gavage) or vehicle for three weeks. After discontinuing treatment, a subset of the mice were monitored for white blood cell (WBC) counts, engraftment rates and survival; another subset of mice were euthanized and BM cells from the femurs of the treated mice were pooled and transplanted into irradiated (6Gy) normal wt recipient mice (B6-Ly5.1, 10^6 cells/mouse). The recipient mice were monitored for WBC counts, engraftment rates and survival.

Statistical analysis

Comparison for two groups was examined by Student's t-test. The log-rank test was used to assess significant differences between survival curves. All statistical analyses were performed using Prism version 8.0 software (GraphPad Software). *In vivo* experiments were performed using 6–15 mice in each group. All *in vitro* experiments were performed in triplicate or more. For all cases, statistical significance was set as $P<0.05$. Results shown represent mean ± SEM. *$P < 0.05$, **$P < 0.01$, ***$P < 0.001$ and ****$P < 0.0001$.

Results

Spred1 deficit promotes CML transformation

To investigate the role of *Spred1* in CML, we first compared SPRED1 expression in BM and CD34$^+$ cells from patients with CP and BC CML. We observed a lower expression of SPRED1 in CD34$^+$ cells by Q-RT-PCR and western blot and in BM by immunohistochemistry (IHC) staining (Fig. 1A, left) from patients with BC CML compared with those from patients with CP CML. Conversely, the expression of miR-126, which targets Spred1[16, 22–24], was higher in both CD34$^+$ and CD34$^+$CD38$^-$ cells from patients

with BC CML compared to the counterparts from patients with CP CML (Fig. 1A, right). We have recently reported that Spred1 blocks miR-126 biogenesis by inhibiting the formation of the RAN-XOP5 complex[16]. Accordingly, we showed that SPRED1 knock-down (KD) by siRNA increased miR-126 expression, quiescence (Fig. 1B) and colony-forming cells (CFC, Fig. 1C) in human CML $CD34^+$ and $CD34^+CD38^-$ cells.

Having discovered lower expression of SPRED1 in BM and $CD34^+$ cells from patients with BC CML, we then hypothesized a functional role of this protein in CML evolution. To prove this hypothesis, we created a new *Spred1* KO CML (i.e., *Spred1*$^{-/-}$*SCLtTA/BCR-ABL*) mouse strain by crossing the inducible *SCLtTA/BCR-ABL* mouse, a well characterized model of CP CML[17, 18], with the *Spred1*$^{-/-}$ mouse[19] (Fig. 2A). Upon confirmation of *Spred1* gene depletion (Supplementary Fig. 1A), BCR-ABL expression was induced in the *Spred1*$^{-/-}$*SCLtTA/BCR-ABL* offspring by tet withdrawal (Fig. 2B, top). Four weeks post BCR-ABL induction, we observed significantly higher WBC counts, an increase in blood and BM leukemic blasts counted by microscopy and an increase in LSKs and granulocyte-macrophage progenitors (GMPs, Lin-Sca1-cKit+CD34+FcγRII/II^{hi}) by flow cytometry (Fig. 2B, middle), two subpopulations that were enriched in leukemic blasts as assessed by microscopy, in the *Spred1*$^{-/-}$*SCLtTA/BCR-ABL* mice compared with *Spred1* wt CML mice. The *Spred1*$^{-/-}$*SCLtTA/BCR-ABL* CML mice also had larger spleens, increased numbers of splenic LSKs and GMPs (Fig. 2B, bottom) and significantly shorter survival (median survival: 26 vs 78 days; $p<0.0001$; Fig. 2C) compared to *Spred1* wt CML mice. A higher fraction of *Spred1*$^{-/-}$*SCLtTA/BCR-ABL* CML mice also developed pro-B lymphoblasts ($B220^+CD43^+CD19^+IgM^-$)-infiltrated lymphadenopathies compared with *Spred1* wt CML mice (33% vs 10%; Supplementary Fig. 1B).

These changes, suggestive of CP evolution into AP and myeloid or lymphoid BC, were also recapitulated in secondary transplant experiments. Congenic normal wt mice engrafted with BM mononuclear cells (MNCs) from leukemic *Spred1*$^{-/-}$*SCLtTA/BCR-ABL* CML mice (BCR-ABL was induced for three weeks by tet withdrawal) had higher WBC counts and blood engraftment rates measured at two weeks after transplantation, increased BM leukemic blasts when moribund, and shorter survival (median survival: 17.5 vs 52 days; $p<0.0001$; Fig. 3A–B) compared to recipients engrafted with BM MNCs from Spred1 wt CML mice. Similar results were also observed when BM LSKs, rather than unsorted BM MNCs, were utilized for the transplant (Fig. 3C).

Taken altogether, these results support that SPRED1 insufficiency contributes to the evolution of CP CML into a more aggressive disease phenotype (i.e., AP/BC CML). The *Spred1*-dependent disease transformation likely occurred at the level of LSCs, as the phenotype observed in primary leukemic *Spred1*$^{-/-}$*SCLtTA/BCR-ABL* mice was recapitulated in secondary normal wt recipients transplanted with *Spred1*$^{-/-}$*SCLtTA/BCR-ABL* BM or LSK cells.

Spred1 insufficiency in HSCs caused an attenuated CML transformation phenotype

Next, we asked if SPRED1 KO restricted only to the hematopoietic compartment of the BM niche was also sufficient to induce CML transformation. To this end, we created a mouse model with a conditional hematopoietic KO by crossing the SCLtTA/BCR-ABL

mouse with a *Spred1$^{f/f}$Mx1-Cre+* (Spred1 KO in hematopoietic cells, hereafter called Spred1$^{HSC\Delta/\Delta}$) mouse. We obtained *SCLtTA/BCR-ABL/Spred1$^{f/f}$/Mx1-Cre+* (hereafter called *Spred1*$^{HSC\Delta/\Delta}$*SCLtTA/BCR-ABL* or *Spred1*$^{HSC\Delta/\Delta}$ CML or HSC-Spred1 KO CML) offspring (Fig. 4A). At eight weeks of age, we induced *Spred1* KO with poly(I:C) administration (250 μg/dose; ip, every 2 days x 7 doses) and BCR-ABL expression by tet withdrawal (Fig. 4B) in these mice. *SCLtTA/BCR-ABL/Spred1$^{f/f}$/Mx1*-Cre-negative (−) (i.e., Spred1 wt CML) control mice were also treated with poly(I:C) and withdrawal of tet.

Four weeks after induction of SPRED1 KO and BCR-ABL expression, the conditional HSC-Spred1 KO CML (i.e., *Spred1$^{HSC\Delta/\Delta}$SCLtTA/BCR-ABL*) mice were found to have higher WBC counts, increased numbers of circulating (blood) blasts, LSKs, GMPs (Fig. 4B) and myeloid cells (Supplementary Fig. 2A), increased numbers of BM blasts, LSKs and GMPs, larger spleens, and increased numbers of splenic LSKs and GMPs (Fig. 4B) compared with the Spred1 wt CML mice. *Spred1$^{HSC\Delta/\Delta}$SCLtTA/BCR-ABL* mice had also a significantly shorter survival than Spred1 wt CML mice (median survival: 51 vs 86 days, p=0.019; Fig. 4C, left). LSKs from poly(I:C)-treated and BCR-ABL-induced (three weeks after tet withdrawal) *Spred1$^{HSC\Delta/\Delta}$SCLtTA/BCR-ABL* mice recapitulated these changes when transplanted into congenic wt recipient mice (Supplementary Fig. 2B–D). All these phenotypic changes were indicative of the evolution of CP CML into a more aggressive phase of the disease (AP/BC).

Interestingly, however, the observed leukemic phenotype of the *Spred1$^{HSC\Delta/\Delta}$SCLtTA/BCR-ABL* mouse was less aggressive than that of the global Spred1 KO CML (*Spred1$^{-/-}$SCLtTA/BCR-ABL*) mouse (median survival: 51 vs 26 days, p=0.0093; Fig. 4C, right). This observation led us to postulate a contribution of Spred1 insufficiency in BM non-hematopoietic compartments during CML transformation.

Spred1 KO in the BM vascular compartment of the BM niche independently contributes to CML transformation

SPRED1 is involved in EC differentiation and formation of vascular and lymphatic vessels via VEGF signaling during organized angiogenesis[22–25]. Aberrant *Spred1* overexpression disrupts vascular integrity both in zebrafish and mice[22, 24]. In mice with EC-specific *Spred1* KO (i.e., Spred1$^{f/f}$Tie2-cre+, hereafter called Spred1$^{EC\Delta/\Delta}$)[20], we observed a significant increase in Sca-1^{high} ECs which line arteriolar vessels in the BM niche (Supplementary Fig. 3A–B). Recent reports have shown that arterioles support homeostasis and quiescence of “self-renewal” HSCs[26–28]. Accordingly, we observed an increased frequency of the quiescent subfraction in BM LT-HSCs (i.e., CD150^{+}CD48^{-}LSK; Supplementary Fig. 3C–D) in Spred1$^{EC\Delta/\Delta}$ compared to Spred1 wt mice. Thus, we postulated that the increase in BM Sca-1^{high} ECs and arterioles associated with EC-Spred1 KO contributes to expansion of LSCs and in turn to CML CP evolution into a more aggressive phase of the disease.

To test this hypothesis, we created an EC-specific Spred1 KO BCR-ABL (hereafter called *Spred1$^{EC\Delta/\Delta}$SCLtTA/BCR-ABL* or Spred1$^{EC\Delta/\Delta}$ CML or EC-Spred1 KO CML) mouse strain by crossing SCLtTA/BCR-ABL with EC-Spred1 KO (i.e., Spred1$^{EC\Delta/\Delta}$) mice (Fig. 5A). In these mice, we observed an increase in both Sca-1^{high} ECs and arterioles (Fig. 5B–C) and a decrease in vascular permeability (Supplementary Fig. 3E) compared to Spred1

wt CML controls. Notably, despite the Spred1 deficit being restricted to the vascular rather than the hematopoietic compartment, *Spred1*$^{EC\Delta/\Delta}$*SCLtTA/BCR-ABL* mice showed signs of CML evolution into AP/BC, as observed in the global Spred1 KO *SCLtTA/BCR-ABL* and *Spred1*$^{HSC\Delta/\Delta}$*SCLtTA/BCR-ABL* mice. Upon BCR-ABL induction by tet withdrawal (Fig. 6A), *Spred1*$^{EC\Delta/\Delta}$*SCLtTA/BCR-ABL* mice had higher WBC counts, increased circulating and BM blasts, increased blood, BM and splenic LSKs and GMPs, larger spleens (Fig. 6B), and shorter survival (median: 54 vs 83 days, p=0.004; Fig. 6C, left) than Spred1 wt CML mice. We also noted that, upon BCR-ABL induction, the *Spred1*$^{EC\Delta/\Delta}$*SCLtTA/BCR-ABL* mice had a median survival similar to Spred1$^{HSC\Delta/\Delta}$SCLtTA/BCR-ABL mice (56 vs 50 days; p=0.72), but longer than global Spred1 KO CML mice (56 vs 26 days; p<0.0001; Fig. 6C, right).

To confirm that these effects were due to Spred1 loss in ECs, and not to a "leaky" *Spred1* downregulation in the hematopoietic compartment, we then transplanted LSKs from the leukemic BCR-ABL mice (B6-Ly5.1/5.2, BCR-ABL induced for three weeks by tet withdrawal) into *Spred1*$^{EC\Delta/\Delta}$ and wt recipient mice (B6-Ly5.2)(Fig. 7A). Spred1$^{EC\Delta/\Delta}$ recipient mice engrafted with LSKs from diseased *SCLtTA/BCR-ABL* mice had higher WBC counts, more CD31^{+}Sca-1^{high} EC-lined arterioles and shorter survival (median: 100 vs 185 days, p=0.027; Fig. 7A; Supplementary Fig. 4A–B) than Spred1 wt recipient mice engrafted with LSKs from diseased *SCLtTA/BCR-ABL* donors.

Notably, we also observed that BM LSKs from *Spred1*$^{EC\Delta/\Delta}$*SCLtTA/BCR-ABL* mice recapitulated these findings when engrafted in congenic normal wt recipients (Fig. 7B). BM LSKs from *Spred1*$^{EC\Delta/\Delta}$*SCLtTA/BCR-ABL* mice induced higher WBC counts, higher blood engraftment rates (Fig. 7B) and LSK numbers (Supplementary Fig. 4C–D) measured at four weeks after transplantation, more BM blasts (Fig. 7B) when moribund, and shorter survival (median: 30 vs 74 days, p<0.0001; Fig. 7B) in recipient mice than BM LSKs from Spred1 wt *SCLtTA/BCR-ABL* mice, supporting the view that even when restricted to ECs, Spred1 KO could affect the burden and activity of LSCs.

Taken altogether these results suggest that EC-Spred1 insufficiency induced a remodeling of the BM vascular niche with increased Sca-1^{high} ECs which safeguard and expand LSCs.

Spred1 depletion in CML promotes TKI resistance

One of the clinical features of the evolution of CML from CP into AP/BC is the acquisition of a relative resistance to TKIs. Thus, to test if SPRED1 KO CML mice also developed a decreased response to TKIs compared with SPRED1 wt CML mice, we first treated BM LSKs from diseased *Spred1*$^{HSC\Delta/\Delta}$ CML or Spred1 wt CML mice (BCR-ABL was induced for four weeks by tet withdrawal) with the TKI NIL (5μM) for 48 hours (hrs). We observed reduced apoptosis in LSKs from *Spred1*$^{HSC\Delta/\Delta}$ CML mice compared with those from Spred1 wt CML mice (Supplementary Fig. 5A). We then transplanted BM cells from Cre+ and Cre- poly(I:C)-treated and BCR-ABL-induced (three weeks after tet withdrawal) *SCLtTA/BCR-ABL/Spred1*$^{f/f}$*/Mx1-Cre* mice into irradiated normal wt recipient mice. Two weeks after transplantation, mice were treated with NIL (50mg/kg/day, oral garage) or vehicle for three weeks (Fig. 8A). Higher WBC counts and blood engraftment rates measured at four weeks after transplantation and shorter survival (Median: 58.5 days vs

unreached after monitoring for 138 days after transplantation; P=0.0009) were observed in NIL-treated HSC-Spred1 KO CML mice compared with NIL-treated Spred1 wt CML mice (Fig. 8A). Of note, NIL treatment significantly enhanced survival in Spred1 wt CML mice (median survival: unreached vs 85 days after monitoring for 138 days after transplantation, P=0.015; Fig. 8A), but not in HSC-Spred1 KO CML mice (median survival: 58 vs 41 days, p=0.078; Fig. 8A) compared to respective vehicle-treated controls.

To determine if Spred1 deficit restricted to the vascular compartment could also attenuate the hematologic response to TKIs in CML mice, we then treated a cohort of Cre+ and Cre- *SCLtTA/BCR-ABL/Spred1$^{f/f}$/Tie2-Cre* mice starting at two weeks post BCR-ABL induction with the TKI NIL (50mg/kg/day, oral gavage) or vehicle for three weeks and then monitored them for WBC counts and survival after discontinuation of treatment. Another cohort of mice were euthanized after three weeks of TKI treatment to assess leukemia burden. Furthermore, BM MNCs from these treated mice were transplanted into normal wt recipient mice (2nd transplantation; Fig. 8B). *Spred1$^{EC\Delta/\Delta}$SCLtTA/BCR-ABL* mice treated with NIL showed higher WBC counts (Fig. 8B), increased BM and splenic LSKs and GMPs (Supplementary Fig. 5B–C), larger spleen (Supplementary Fig. 5D), and shorter survival (median: 27 vs 48.5 days, P=0.02; Fig. 8B) than Spred1 wt CML mice treated with NIL. Recipients of BM MNCs from NIL-treated *Spred1$^{EC\Delta/\Delta}$SCLtTA/BCR-ABL* mice also showed higher WBC counts and blood engraftment rates and shorter survival (median: 116 vs 187 days; P=0.0035) than recipients of BM MNCs from NIL-treated Spred1 wt CML mice (Fig. 8B), suggesting higher post-treatment LSC burden in these mice. Taken altogether, these results support a role of Spred1 deficit in non-hematopoietic compartments of the leukemic BM niche in acquired CML TKI resistance.

Mechanistic aspects of SPRED1 deficit in CML

Having shown that Spred1 KO contributes to CML transformation, we next dissected the molecular mechanisms involved in this process. To this end, we recently showed that, in LSCs, SPRED1 inhibits the activity of RAN, a RAS family member that regulates miRNA biogenesis[16]. RAN binds to XPO5 to form a complex that permits transportation of pre-miRNAs from the nucleus to the cytoplasm for the last step of miRNA maturation[16]. SPRED1 deficit removes the inhibition on the RAN-XPO5 complex and allows pre-miR-126 to be transported from the nucleus to the cytoplasm where it is converted into mature miR-126. Accordingly, herein, we showed higher levels of mature miR-126 in BM LSKs from *Spred1$^{HSC\Delta/\Delta}$* CML mice compared to those from Spred1 wt CML mice (Supplementary Fig. 6A).

We also observed similar findings in ECs, *in vitro* in human umbilical vein endothelial cells (HUVECs) and murine BM ECs using siRNA to achieve Spred1 KD (Supplementary Fig. 6B–C), and *in vivo* in BM ECs from *Spred1$^{EC\Delta/\Delta}$* CML mice (Supplementary Fig. 6D), suggesting similar, rather than cell-specific, Spred1-driven molecular mechanisms in both LSKs and ECs. As ECs supply miR-126 to LSCs by extracellular vesicles[16], we also observed increased levels of mature miR-126 in BM LSKs from EC-Spred1 KO CML mice compared to those from Spred1 wt CML mice (Supplementary Fig. 6E). Thus, Spred1 KO

in either LSKs or ECs, ultimately resulted in increased miR-126 in LSKs, which under these conditions expanded.

Having shown that both HSC-Spred1 KO and EC-Spred1 KO ultimately increased miR-126 in LSKs, we next performed RNA-seq on LSKs from *Spred1*$^{HSC\Delta/\Delta}$*SCLtTA/BCR-ABL* (HSC KO), *Spred1*$^{EC\Delta/\Delta}$*SCLtTA/BCR-ABL* (EC KO) and their respective *Spred1* wt control mice (n=5 mice per group, Supplementary Fig. 7) to assess whether similar molecular changes also occurred in this LSC-enriched population. Remarkably, by gene set enrichment analysis (GSEA), LSKs from both *Spred1*$^{HSC\Delta/\Delta}$*SCLtTA/BCR-ABL* (Supplementary Fig. 8A–C, 9) and *Spred1*$^{EC\Delta/\Delta}$*SCLtTA/BCR-ABL* (Supplementary Fig. 10A–C, 11) mice showed similar profiles. Oxidative phosphorylation (OxPhos) was one of the most upregulated cell processes. We functionally validated this finding by performing Seahorse metabolic assays on LSKs from both Spred1 KO (i.e., HSC KO and EC KO) CML models vs those from Spred1 wt CML controls (Supplementary Fig. 12A). In LSKs from both models, OxPhos was significantly enhanced compared with those from Spred1 wt CML controls as demonstrated by the changes in oxygen consumption rate (OCR).

Notably, in LSCs, OxPhos is Bcl-2-depedent[29]. It is known that Spred1 interacts with neurofibromin to inhibit the MAPK/ERK pathway[6], which provides a signal not only for cell proliferation but also for cell survival by increasing phospho (p)-Bcl-2 levels[30, 31]. To this end, since Spred1 deficit (caused by direct Spred1 KO in LSKs or increased miR-126 supply to LSKs from Spred1 KO ECs) removed inhibition of the MAPK/ERK pathway, higher levels of both p-Erk and p-Bcl-2 were observed in LSKs from both *Spred1*$^{HSC\Delta/\Delta}$*SCLtTA/BCR-ABL* and *Spred1*$^{EC\Delta/\Delta}$*SCLtTA/BCR-ABL* CML mice compared with Spred1 wt CML controls (Supplementary Fig. 12B).

Taken altogether, these data suggest that Spred1 deficit increases miR-126 production in both LSKs and ECs in CML mice through similar mechanisms (i.e., hyperactivation of RAN/XPO5 complex). Spred1 KO ECs supply miR-126 to LSKs, where it targets and reduces endogenous Spred1. Therefore, Spred1 deficit results in miR-126 OE in LSKs, regardless if achieved intrinsically by HSC-Spred1 KO or extrinsically by EC-Spred1 KO. These changes ultimately lead to hyperactivation of the MAPK/ERK pathway and a higher and more efficient Bcl-2-dependent OxPhos that supports the homeostasis, survival and activity of LSCs, hence disease transformation.

Discussion

The molecular mechanisms of transformation of CP CML into AP/BC CML remain to be fully elucidated. While previous studies have focused on factors, such as i) progressive increase of BCR-ABL levels over time, ii) acquisition of additional chromosomal and genetic aberrations, and iii) abnormal activation of multiple kinase-driven signaling pathways, to explain the transformation of CP into AP/BC CML[2], the interplay of the hematopoietic and non-hematopoietic compartments of the leukemic BM niche during disease evolution has not been fully evaluated. Herein, we showed that Spred1 KO induced in the hematopoietic or vascular compartment of the leukemic BM niche contributed to the transformation of CP into AP/BC in the CML mouse, and that concurrent deficit in both

compartments were likely to have an additive effect, given the more aggressive phenotype observed in the global SPRED1 KO CML model. While our analysis was limited to the hematopoietic and vascular compartments, these findings do not exclude the possibility that Spred1 deficit in other non-hematopoietic compartments of the BM niche could also contribute to CML transformation.

Spred1 is a verified target and a regulator of miR-126[16]. Thus, Spred1 deficit caused an increase in miR-126, that contributed to the expansion and enhanced activity of LSCs and led to disease transformation[15, 16]. Despite the limited number of large RNA-seq databases publicly available, we were able to show acquisition of SPRED1 deficit in BM and $CD34^+$ cells from patients with BC CML compared with patients with CP CML. In a relatively small series of consecutive cases of patients with CML from our Institution, we showed that SPRED1 mRNA and protein levels were decreased in patients with AP/BC CML, which also expressed high levels of miR-126, compared to patients with CP CML. Importantly, we validated the functional role of SPRED1 deficit in CML transformation showing that global SPRED1 KO induced AP/BC in a CML murine model. Interestingly, Spred1 deficit, restricted either to the hematopoietic or to the vascular compartment of the leukemic BM niche, also induced CP transformation, supporting the notion that mechanisms extrinsic to the hematopoietic compartment are also involved in the natural history of this disease.

Importantly, BM LSKs from HSC-Spred1 KO CML mice transplanted into normal Spred1 wt mice recapitulated the transformed phenotype, supporting the notion that Spred1 deficit induced functional and permanent changes in LSCs from the primary donors. Furthermore, transplants with LSKs from the EC-Spred1 KO CML mouse also recapitulated the transformed phenotype in secondary recipients, suggesting that Spred1 KO restricted to the vascular compartment also induced functional and permanent changes in LSCs from the primary donors. How do we explain these observations mechanistically?

Firstly, we asked whether hematopoietic and vascular SPRED1 KO induced similar molecular changes in LSKs (a cell subpopulation enriched in LSCs). To this end, we performed RNA-seq of LSKs from EC-Spred1 KO and HSC-Spred1 KO CML mice vs their respective Spred1 wt CML controls. Through GSEA, we showed that LSKs from both Spred1 KO CML strains shared similar profiles despite the fact that Spred1 KO was induced in different tissues. Among others, genes involved in OxPhos were significantly enriched. We functionally validated these genomic findings by showing that OxPhos activity was significantly higher in LSKs (i.e., LSCs) from both EC-Spred1 KO and HSC-Spred1 KO CML mice compared to those from their respective Spred1 wt CML controls using Seahorse metabolic assays. It has been extensively reported that LSC homeostasis, survival and activity strictly depend on OxPhos metabolisms[29, 32]. Thus, these functional changes may explain the contribution of Spred1 deficit to the disease transformation as the consequence of a more robust OxPhos metabolism and LSC expansion.

Secondly, we raised the question of how both EC-Spred1 KO and HSC-Spred1 KO in CML mice could induce similar metabolic changes in LSKs. To this end, we have previously reported that Spred1 is an inhibitor of RAN and thus Spred1 deficit causes hyperactivation of the RAN/XPO5 complex[16] thereby enhancing miR-126 biogenesis and in turn increasing

levels of mature miR-126. In fact, Spred1 KO increased the RAN/XPO5 complex and miR-126 levels in both LSKs and ECs. Of note, since ECs supply miR-126 to LSKs via extracellular vesicles (EVs)[16], the net result of the EC-Spred1 KO is an increase of miR-126 in LSKs, similar to what we observed in HSC-Spred1 KO.

Thirdly, we raised the question of how Spred1 KO and in turn miR-126 up-regulation could enhance OxPhos in LSKs. Given that Spred1 is also a verified target of miR-126[16, 22–24], upregulated miR-126 in LSKs from both HSC-Spred1 KO and EC-Spred1 KO CML mice through intrinsic (HSC KO) or extrinsic (EC KO) mechanism respectively, led to Spred1 downregulation in LSCs. To this end, it is known that Spred1 is an inhibitor of RAS-MAPK signaling[33, 34] which activates mechanisms of cell proliferation and survival[35]. In both HSC-Spred1 KO and EC-Spred1 KO CML models, SPRED1 downregulation in LSKs resulted in hyperactivation of the RAS/RAF/MEK/ERK pathway and increased levels of Bcl-2, which stabilizes and enhances OxPhos in LSCs[29]. The increase in OxPhos allowed for expansion of LSCs as demonstrated by decreased survival in secondary recipients of LSKs from global, HSC and EC Spred1 KO CML models compared to recipients of LSKs from Spred1 wt CML controls. Of note, we also observed hyperactivated RAS/MAPK/ERK pathway and increased Bcl-2 expression in Spred1 KD HUVECs (by siRNA) and Spred1 KO murine BM ECs (from EC-Spred1 KO mice) compared to Spred1 wt counterparts (not shown). How these molecular changes induce BM enrichment in Sca-1^{high} ECs needs to be further explored.

In conclusion, herein we report on the transforming role of Spred1 deficit in CML likely through LSC expansion. The latter appears to be caused by enhancement of Bcl-2-dependent OxPhos, among other possible and concurrent mechanisms (see GSEA in Supplementary Fig. 8B–C, 10B–C). Importantly, we showed the interplay of the hematopoietic and vascular compartments of the leukemic BM niche, as supported by the fact that Spred1 KO in either compartment induced an attenuated phenotype compared to global Spred1 KO. To this end, our results are somewhat reminiscent of those reported by Tadokoro et al[14]. These authors showed that normal wt recipient mice transplanted with *Spred1*$^{-/-}$ BM cells and fed with HFD developed an attenuated myeloproliferative disorder compared to the germline *Spred1*$^{-/-}$ mice fed with HFD[14].

Taken altogether, our findings indicate that Spred1 deficit is a contributor to CML transformation and therefore a potential new therapeutic target to prevent or treat disease transformation. However, it would be challenging to develop therapeutics that can restore Spred1 levels. Nevertheless, we have previously reported on an anti-miR-126 oligonucleotide (i.e., miRisten) that can effectively upregulate Spred1 in LSCs[16]. Thus, we propose to further explore miR-126 targeting as a potential approach to rescue Spred1 insufficiency in AP/BC CML.

Supplementary Material

Refer to Web version on PubMed Central for supplementary material.

Acknowledgments

This work was supported in part by National Cancer Institute grants: CA248475 (GM/BZ), CA205247 (YHK/GM), CA201184 (GM), CA25004467 (RCR/YHK/GM), the Gehr Family Foundation (GM), the George Hoag Family Foundation (GM), International Program for Ph.D. Candidates (Sun Yat-Sen University, China), JSPS KAKENHI (S) JP17H06175 and AMED-CREST JP 20gm1110009 (AY). We are grateful to Marjorie Robbins for editing the manuscript. We acknowledge the support of the Animal Resources Center, Analytical Cytometry, Pathology (Hematopoietic Tissue Biorepository), Light Microscopy, and DNA/RNA Cores at City of Hope Comprehensive Cancer Center supported by the National Cancer Institute of the National Institutes of Health under award number P30CA33572. We are grateful to COH Comprehensive Cancer Center, the patients, and their physicians for providing primary patient material for this study.

Availability of data and materials

RNA sequencing data produced in our laboratory and analysed in this study are available at the Gene Expression Omnibus (GEO) repository of the National Center for Biotechnology Information (GSE181589). Supplementary information including Supplementary Figures 1–12 and Supplementary table 1 are provided with the online version of this paper. All other datasets generated during this study are available from the corresponding author on reasonable request.

References

1. Rowley JD. Letter: A new consistent chromosomal abnormality in chronic myelogenous leukaemia identified by quinacrine fluorescence and Giemsa staining. Nature 1973 Jun 1; 243(5405): 290–293. [PubMed: 4126434]
2. Perrotti D, Jamieson C, Goldman J, Skorski T. Chronic myeloid leukemia: mechanisms of blastic transformation. J Clin Invest 2010 Jul; 120(7): 2254–2264. [PubMed: 20592475]
3. Karbasian Esfahani M, Morris EL, Dutcher JP, Wiernik PH. Blastic phase of chronic myelogenous leukemia. Curr Treat Options Oncol 2006 May; 7(3): 189–199. [PubMed: 16615875]
4. Kawazoe T, Taniguchi K. The Sprouty/Spred family as tumor suppressors: Coming of age. Cancer Sci 2019 May; 110(5): 1525–1535. [PubMed: 30874331]
5. Quintanar-Audelo M, Yusoff P, Sinniah S, Chandramouli S, Guy GR. Sprouty-related Ena/vasodilator-stimulated phosphoprotein homology 1-domain-containing protein (SPRED1), a tyrosine-protein phosphatase non-receptor type 11 (SHP2) substrate in the Ras/extracellular signal-regulated kinase (ERK) pathway. J Biol Chem 2011 Jul 1; 286(26): 23102–23112. [PubMed: 21531714]
6. Wakioka T, Sasaki A, Kato R, Shouda T, Matsumoto A, Miyoshi K, et al. Spred is a Sprouty-related suppressor of Ras signalling. Nature 2001 Aug 9; 412(6847): 647–651. [PubMed: 11493923]
7. Miyoshi K, Wakioka T, Nishinakamura H, Kamio M, Yang L, Inoue M, et al. The Sprouty-related protein, Spred, inhibits cell motility, metastasis, and Rho-mediated actin reorganization. Oncogene 2004 Jul 22; 23(33): 5567–5576. [PubMed: 15184877]
8. Nguyen LXT, Zhang B, Hoang DH, Zhao D, Wang H, Wu H, et al. Cytoplasmic DROSHA and non-canonical mechanisms of MiR-155 biogenesis in FLT3-ITD acute myeloid leukemia. Leukemia 2021 Aug; 35(8): 2285–2298. [PubMed: 33589748]
9. Brems H, Chmara M, Sahbatou M, Denayer E, Taniguchi K, Kato R, et al. Germline loss-of-function mutations in SPRED1 cause a neurofibromatosis 1-like phenotype. Nat Genet 2007 Sep; 39(9): 1120–1126. [PubMed: 17704776]
10. Pasmant E, Ballerini P, Lapillonne H, Perot C, Vidaud D, Leverger G, et al. SPRED1 disorder and predisposition to leukemia in children. Blood 2009 Jul 30; 114(5): 1131. [PubMed: 19643996]
11. Pasmant E, Gilbert-Dussardier B, Petit A, de Laval B, Luscan A, Gruber A, et al. SPRED1, a RAS MAPK pathway inhibitor that causes Legius syndrome, is a tumour suppressor downregulated in paediatric acute myeloblastic leukaemia. Oncogene 2015 Jan 29; 34(5): 631–638. [PubMed: 24469042]

12. Cancer Genome Atlas Research N, Ley TJ, Miller C, Ding L, Raphael BJ, Mungall AJ, et al. Genomic and epigenomic landscapes of adult de novo acute myeloid leukemia. N Engl J Med 2013 May 30; 368(22): 2059–2074. [PubMed: 23634996]

13. Olsson L, Castor A, Behrendtz M, Biloglav A, Forestier E, Paulsson K, et al. Deletions of IKZF1 and SPRED1 are associated with poor prognosis in a population-based series of pediatric B-cell precursor acute lymphoblastic leukemia diagnosed between 1992 and 2011. Leukemia 2014 Feb; 28(2): 302–310. [PubMed: 23823658]

14. Tadokoro Y, Hoshii T, Yamazaki S, Eto K, Ema H, Kobayashi M, et al. Spred1 Safeguards Hematopoietic Homeostasis against Diet-Induced Systemic Stress. Cell Stem Cell 2018 May 3; 22(5): 713–725 e718. [PubMed: 29706577]

15. Lechman ER, Gentner B, Ng SW, Schoof EM, van Galen P, Kennedy JA, et al. miR-126 Regulates Distinct Self-Renewal Outcomes in Normal and Malignant Hematopoietic Stem Cells. Cancer Cell 2016 Feb 8; 29(2): 214–228. [PubMed: 26832662]

16. Zhang B, Nguyen LXT, Li L, Zhao D, Kumar B, Wu H, et al. Bone marrow niche trafficking of miR-126 controls the self-renewal of leukemia stem cells in chronic myelogenous leukemia. Nat Med 2018 May; 24(4): 450–462. [PubMed: 29505034]

17. Koschmieder S, Gottgens B, Zhang P, Iwasaki-Arai J, Akashi K, Kutok JL, et al. Inducible chronic phase of myeloid leukemia with expansion of hematopoietic stem cells in a transgenic model of BCR-ABL leukemogenesis. Blood 2005 Jan 1; 105(1): 324–334. [PubMed: 15331442]

18. Zhang B, Ho YW, Huang Q, Maeda T, Lin A, Lee SU, et al. Altered microenvironmental regulation of leukemic and normal stem cells in chronic myelogenous leukemia. Cancer Cell 2012 Apr 17; 21(4): 577–592. [PubMed: 22516264]

19. Inoue H, Kato R, Fukuyama S, Nonami A, Taniguchi K, Matsumoto K, et al. Spred-1 negatively regulates allergen-induced airway eosinophilia and hyperresponsiveness. J Exp Med 2005 Jan 3; 201(1): 73–82. [PubMed: 15630138]

20. Ishizaki T, Tamiya T, Taniguchi K, Morita R, Kato R, Okamoto F, et al. miR126 positively regulates mast cell proliferation and cytokine production through suppressing Spred1. Genes Cells 2011 Jul; 16(7): 803–814. [PubMed: 21668589]

21. Kusumbe AP, Ramasamy SK, Starsichova A, Adams RH. Sample preparation for high-resolution 3D confocal imaging of mouse skeletal tissue. Nat Protoc 2015 Dec; 10(12): 1904–1914. [PubMed: 26513669]

22. Fish JE, Santoro MM, Morton SU, Yu S, Yeh RF, Wythe JD, et al. miR-126 regulates angiogenic signaling and vascular integrity. Dev Cell 2008 Aug; 15(2): 272–284. [PubMed: 18694566]

23. Kuhnert F, Mancuso MR, Hampton J, Stankunas K, Asano T, Chen CZ, et al. Attribution of vascular phenotypes of the murine Egfl7 locus to the microRNA miR-126. Development 2008 Dec; 135(24): 3989–3993. [PubMed: 18987025]

24. Wang S, Aurora AB, Johnson BA, Qi X, McAnally J, Hill JA, et al. The endothelial-specific microRNA miR-126 governs vascular integrity and angiogenesis. Dev Cell 2008 Aug; 15(2): 261–271. [PubMed: 18694565]

25. Taniguchi K, Kohno R, Ayada T, Kato R, Ichiyama K, Morisada T, et al. Spreds are essential for embryonic lymphangiogenesis by regulating vascular endothelial growth factor receptor 3 signaling. Mol Cell Biol 2007 Jun; 27(12): 4541–4550. [PubMed: 17438136]

26. Ding L, Saunders TL, Enikolopov G, Morrison SJ. Endothelial and perivascular cells maintain haematopoietic stem cells. Nature 2012 Jan 25; 481(7382): 457–462. [PubMed: 22281595]

27. Itkin T, Gur-Cohen S, Spencer JA, Schajnovitz A, Ramasamy SK, Kusumbe AP, et al. Distinct bone marrow blood vessels differentially regulate haematopoiesis. Nature 2016 Apr 21; 532(7599): 323–328. [PubMed: 27074509]

28. Kunisaki Y, Bruns I, Scheiermann C, Ahmed J, Pinho S, Zhang D, et al. Arteriolar niches maintain haematopoietic stem cell quiescence. Nature 2013 Oct 31; 502(7473): 637–643. [PubMed: 24107994]

29. Lagadinou ED, Sach A, Callahan K, Rossi RM, Neering SJ, Minhajuddin M, et al. BCL-2 inhibition targets oxidative phosphorylation and selectively eradicates quiescent human leukemia stem cells. Cell Stem Cell 2013 Mar 7; 12(3): 329–341. [PubMed: 23333149]

30. Boucher MJ, Morisset J, Vachon PH, Reed JC, Laine J, Rivard N. MEK/ERK signaling pathway regulates the expression of Bcl-2, Bcl-X(L), and Mcl-1 and promotes survival of human pancreatic cancer cells. J Cell Biochem 2000 Sep 7; 79(3): 355–369. [PubMed: 10972974]

31. Galante JM, Mortenson MM, Bowles TL, Virudachalam S, Bold RJ. ERK/BCL-2 pathway in the resistance of pancreatic cancer to anoikis. J Surg Res 2009 Mar; 152(1): 18–25. [PubMed: 19062038]

32. Kuntz EM, Baquero P, Michie AM, Dunn K, Tardito S, Holyoake TL, et al. Targeting mitochondrial oxidative phosphorylation eradicates therapy-resistant chronic myeloid leukemia stem cells. Nat Med 2017 Oct; 23(10): 1234–1240. [PubMed: 28920959]

33. Bundschu K, Walter U, Schuh K. Getting a first clue about SPRED functions. Bioessays 2007 Sep; 29(9): 897–907. [PubMed: 17691106]

34. Yoshimura A Regulation of cytokine signaling by the SOCS and Spred family proteins. Keio J Med 2009 Jun; 58(2): 73–83. [PubMed: 19597303]

35. Lorenzo C, McCormick F. SPRED proteins and their roles in signal transduction, development, and malignancy. Genes Dev 2020 Nov 1; 34(21–22): 1410–1421. [PubMed: 33872193]

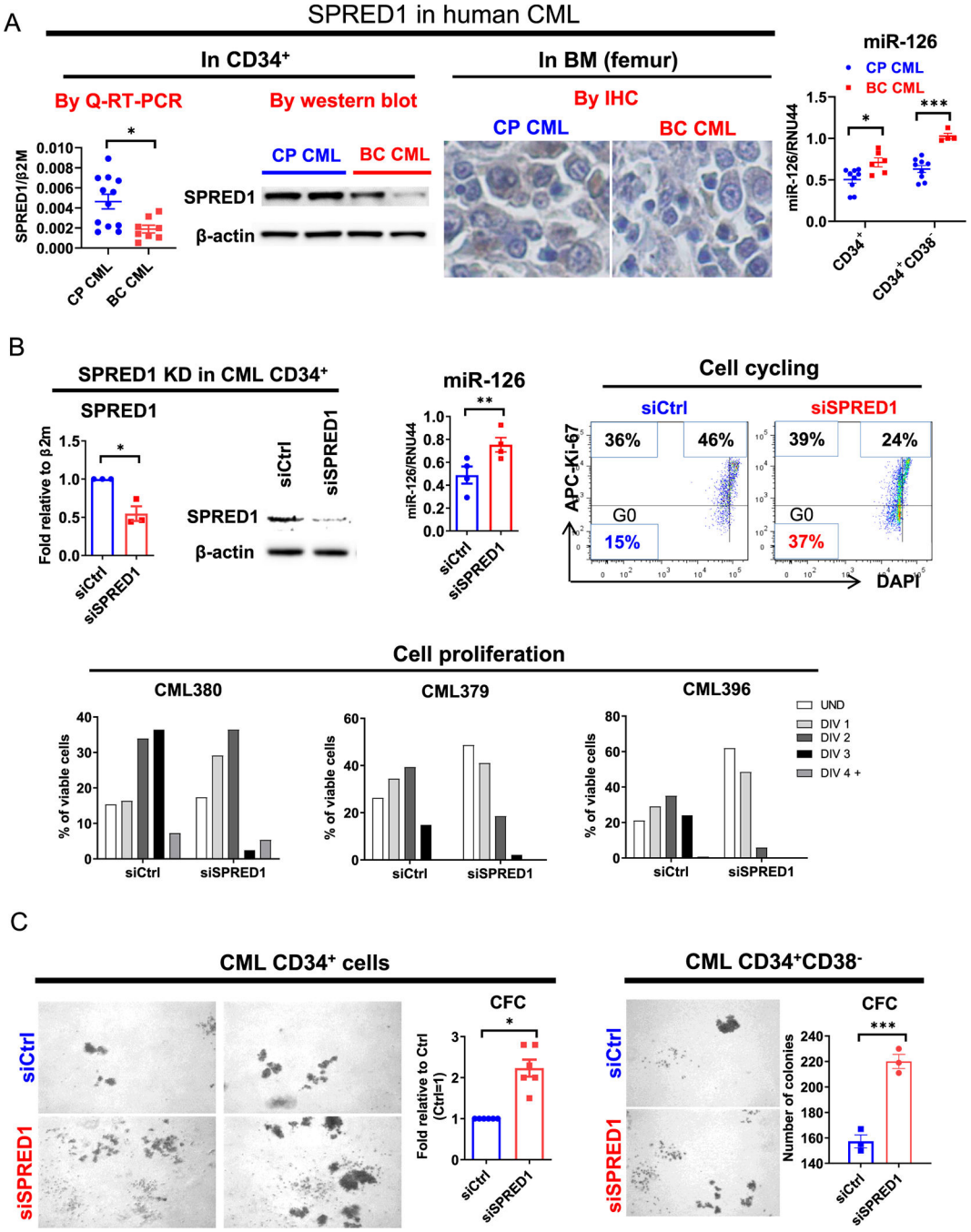

Figure 1. Downregulation of Spred1 was observed in BM and CD34$^+$ cells from patients with BC CML and associated with an increased "stemness" phenotype.

A Expression of SPRED1 in BM CD34$^+$ cells from patients with BC CML and CP CML by Q-RT-PCR (n=8 samples for BC CML and n=12 samples for CP CML) and western blot and in BM by immunohistochemistry staining (one of three independent experiments with similar results was shown) (left), and expression of miR-126 in CD34$^+$ and CD34$^+$CD38$^-$ cells from BC CML (n=6 samples) and CP CML (n=10 samples) patients by Q-RT-PCR (right). **B** SPRED1 mRNA expression by Q-RT-PCR and protein expression by western blot,

miR-126 levels by Q-RT-PCR, cell cycling by Ki-67 and DAPi staining (top) or by cell trace violet staining (bottom) followed by flow cytometry analysis in CML $CD34^+$ cells transduced with SPRED1 siRNA to knock-down (KD) SPRED1 or with a non-targeting control siRNA (Ctrl). UND: undivided cells, G0; DIV: division. **C** Representative colonies and quantification of colony forming cells (CFC) in CML $CD34^+$ (left) and $CD34^+CD38^-$ (right) cells transduced with Spred1 siRNA to KD SPRED1 or with ctrl siRNA (n=3). Results shown represent mean ± SEM. Significance values: *, $p<0.05$; **, $p<0.01$; ***, $p<0.001$.

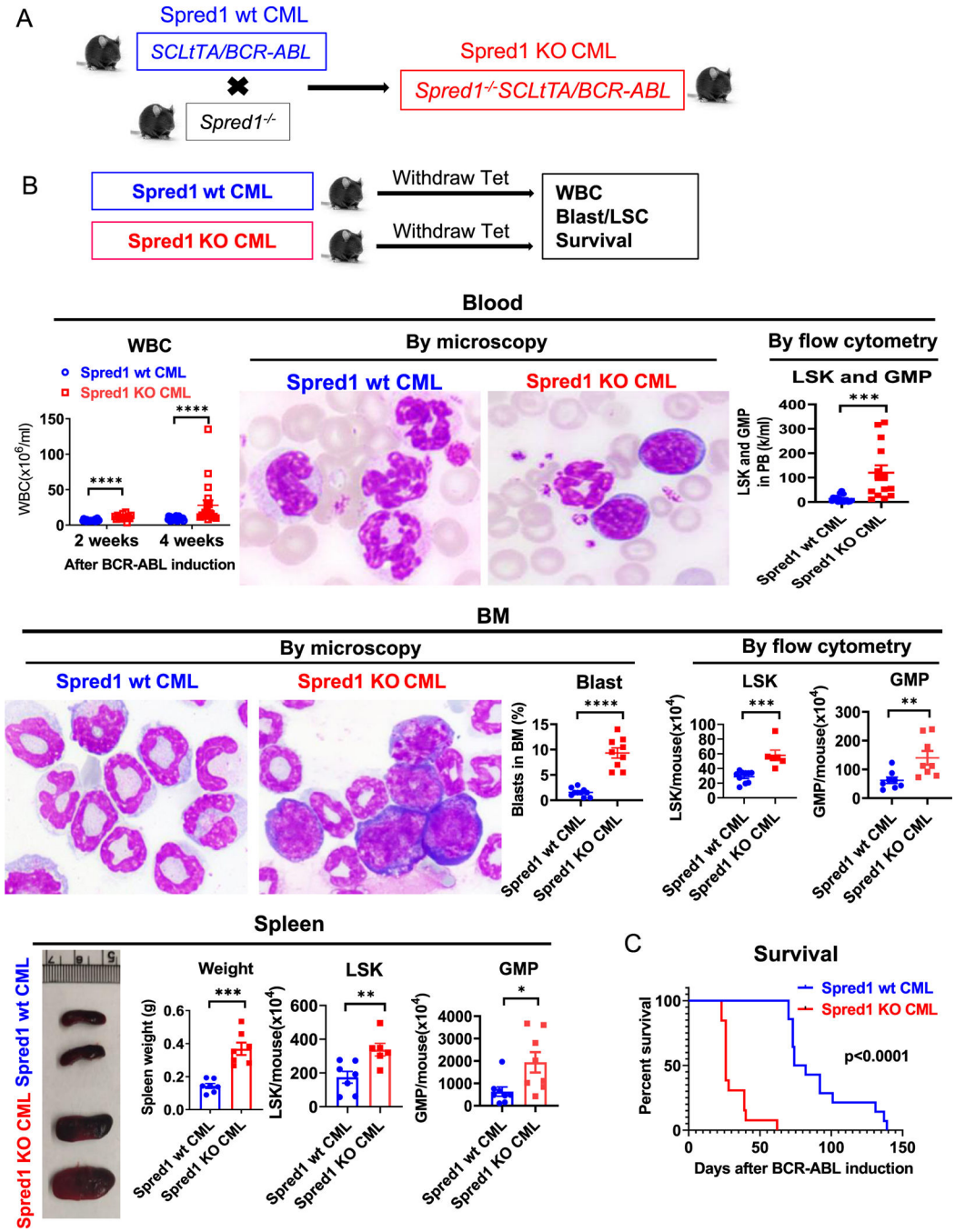

Figure 2. Spred1 deficit promotes CML transformation.

A Schematic design of the mouse crossings. **B** Schematic design and results of the experiments. After tetracycline withdrawal to induce BCR-ABL expression, Spred1 wt SCLtTA/BCR-ABL and Spred1 KO SCLtTA/BCR-ABL mice (n=15 mice per group) were monitored for white blood cell (WBC) counts in peripheral blood (PB) every two weeks. Four weeks post BCR-ABL induction, blood and BM leukemic blasts by microscopy and LSKs and GMPs by flow cytometry, spleen size and weight, and splenic LSKs and GMPs by flow cytometry, in the Spred1 KO CML mice were compared with Spred1 wt CML

mice. **C** Survival of Spred1 wt SCLtTA/BCR-ABL and Spred1 KO SCLtTA/BCR-ABL mice after BCR-ABL induction (n=10 mice per group). Results shown represent mean ± SEM. Significance values: *, $p<0.05$; **, $p<0.01$; ***, $p<0.001$; ****, $p<0.0001$.

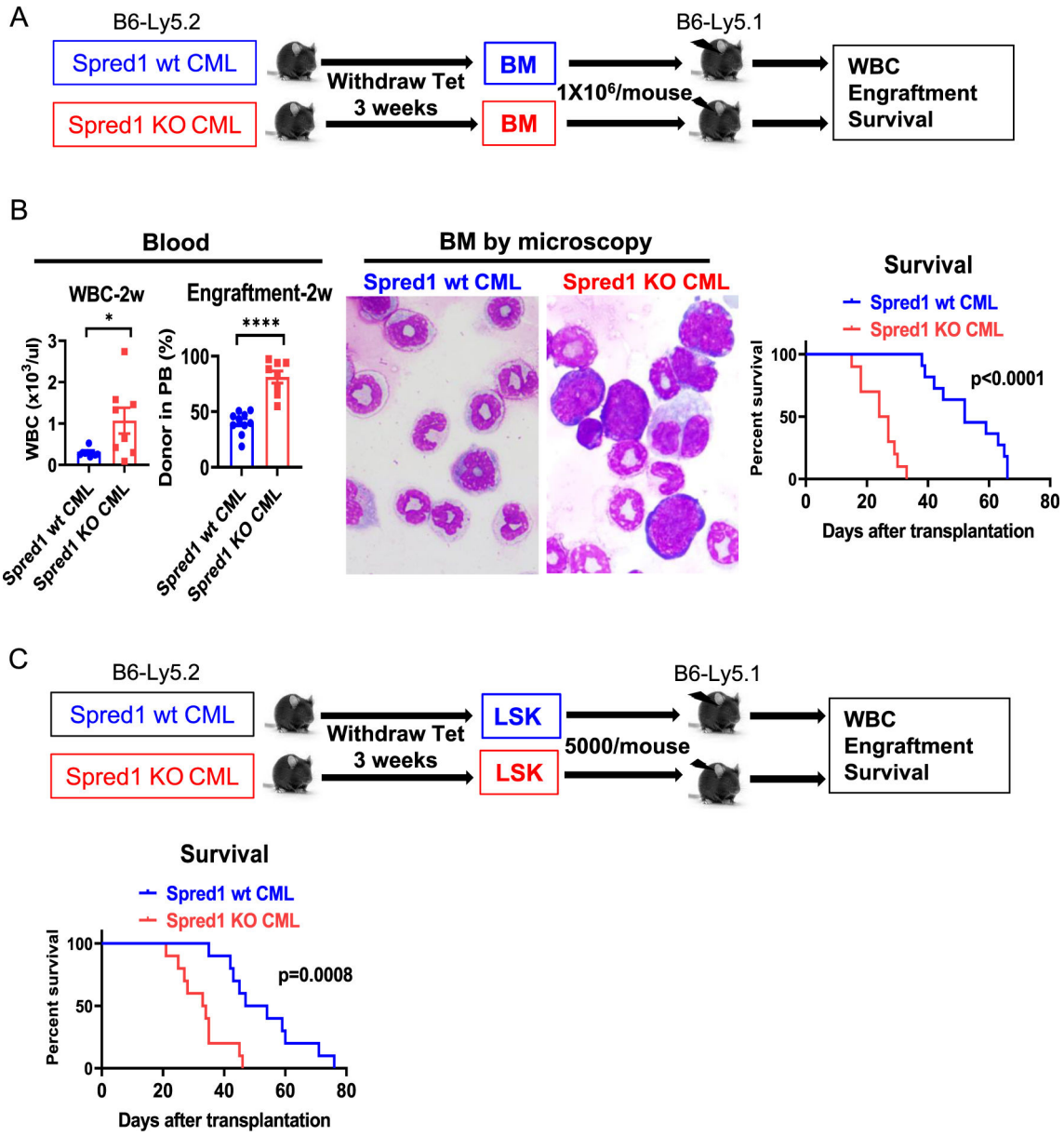

Figure 3. BM or LSK cells from Spred1 KO CML mice recapitulated AP/BC phenotype in recipient mice.

A Schematic design of the experiments. Three weeks after tetracycline withdrawal to induce BCR-ABL expression, BM MNCs from Spred1 wt SCLtTA/BCR-ABL and Spred1 KO SCLtTA/BCR-ABL mice (B6-Ly5.2, n=3 mice per group) were selected and transplanted into congenic normal wt recipient mice (B6-Ly5.1, n=10 mice per group), followed by measurement of WBC counts, engraftment and survival. **B** WBC counts, blood CML engraftment rates analyzed by flow cytometry (left), BM leukemic blasts by microscopy (middle), and survival (right) of recipient mice transplanted with BM MNCs from Spred1 wt CML or from Spred1 KO CML mice. **C** Schematic design and results of the experiments. After three weeks of BCR-ABL induction by tetracycline withdrawal, BM LSKs from Spred1 wt SCLtTA/BCR-ABL and Spred1 KO SCLtTA/BCR-ABL mice (B6-Ly5.2, n=3

mice per group) were selected and transplanted into congenic normal wt recipient mice (B6-Ly5.1, n=10 mice per group) and survival of the recipient mice was shown. Results shown represent mean ± SEM. Significance values: *, $p<0.05$; ****, $p<0.0001$.

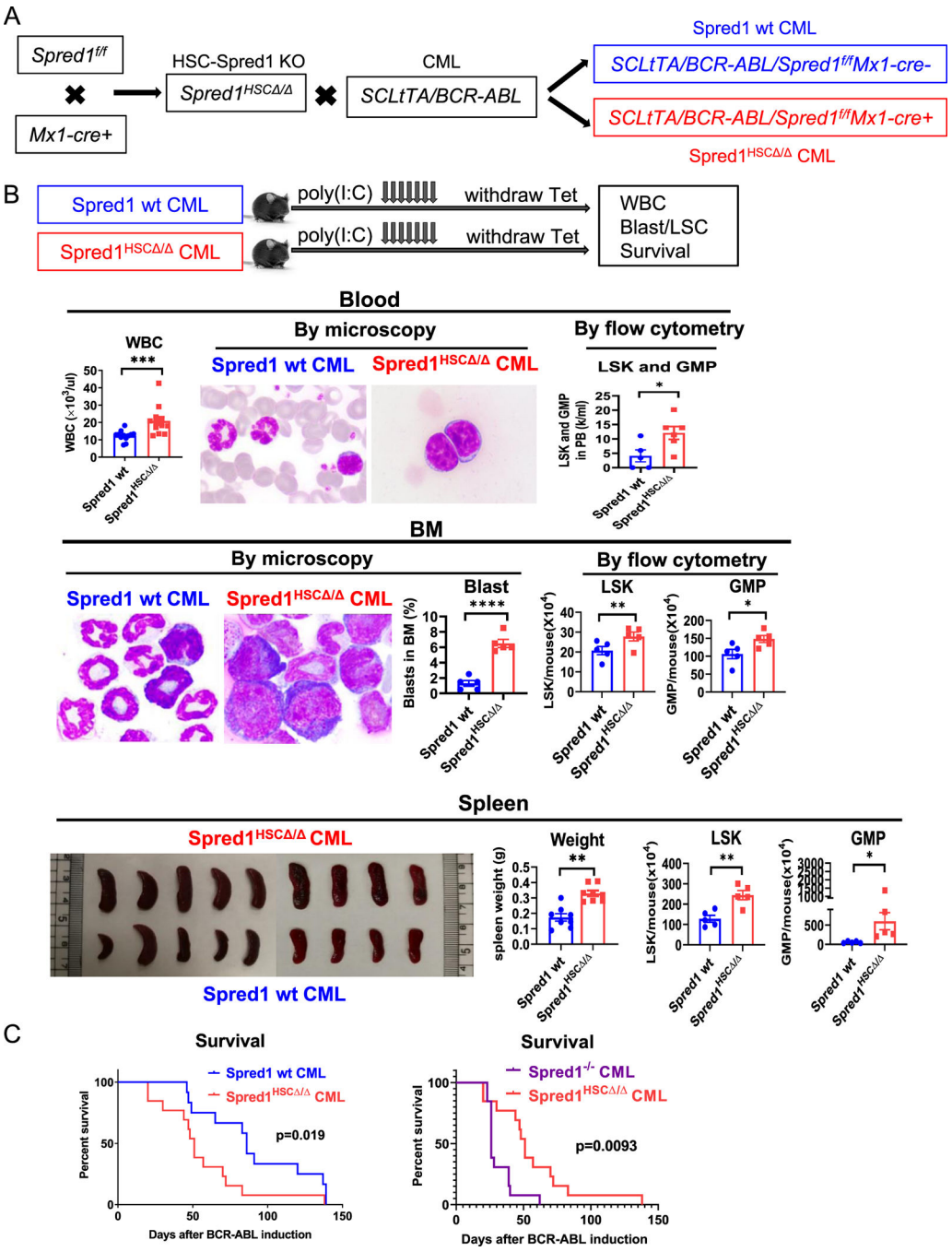

Figure 4. *Spred1* insufficiency in HSCs caused an attenuated CML transformation phenotype.
A Schematic design of the mouse crossing. *Spred1*$^{flox(f)/f}$ (B6-Ly5.2) mouse was crossed with Mx1-Cre+ (B6-Ly5.2; Jax lab, #2527) mouse to generate Spred1$^{f/f}$Mx1-Cre+ (Spred1 KO in HSCs, hereafter called Spred1$^{HSC\Delta/\Delta}$) mice. Spred1$^{f/f}$Mx1-Cre+ mice were then bred with SCLtTA/BCR-ABL mice to obtain SCLtTA/BCR-ABL/Spred1$^{f/f}$Mx1-Cre+ (Spred1$^{HSC\Delta/\Delta}$ SCLtTA/BCR-ABL) or Cre- (Spred1 wt SCLtTA/BCR-ABL) mice. **B** Schematic design and results of the experiments. Spred1 wt SCLtTA/BCR-ABL and Spred1$^{HSC\Delta/\Delta}$SCLtTA/BCR-ABL mice were treated with 7 doses of poly(I:C) to activate

Cre activity, followed by tetracycline withdrawal to induce BCR-ABL expression (n=12 mice per group). WBC counts, blood and BM leukemic blasts by microscopy and LSKs and GMPs by flow cytometry, spleen size and weight and LSK and GMP numbers by flow cytometry in Spred1 wt CML and Spred1$^{HSC\Delta/\Delta}$ CML mice measured at four weeks after poly(I:C) administration and BCR-ABL induction. **C** Survival of Spred1 wt SCLtTA/BCR-ABL and Spred1$^{HSC\Delta/\Delta}$SCLtTA/BCR-ABL mice after poly(I:C) administration and BCR-ABL induction (left) and survival of Spred1$^{HSC\Delta/\Delta}$SCLtTA/BCR-ABL (HSC-Spred1 KO) and Spred1$^{-/-}$SCLtTA/BCR-ABL (global KO) after BCR-ABL induction (n=13 mice per group). Results shown represent mean ± SEM. Significance values: *, $p<0.05$; **, $p<0.01$; ***, $p<0.001$; ****, $p<0.0001$.

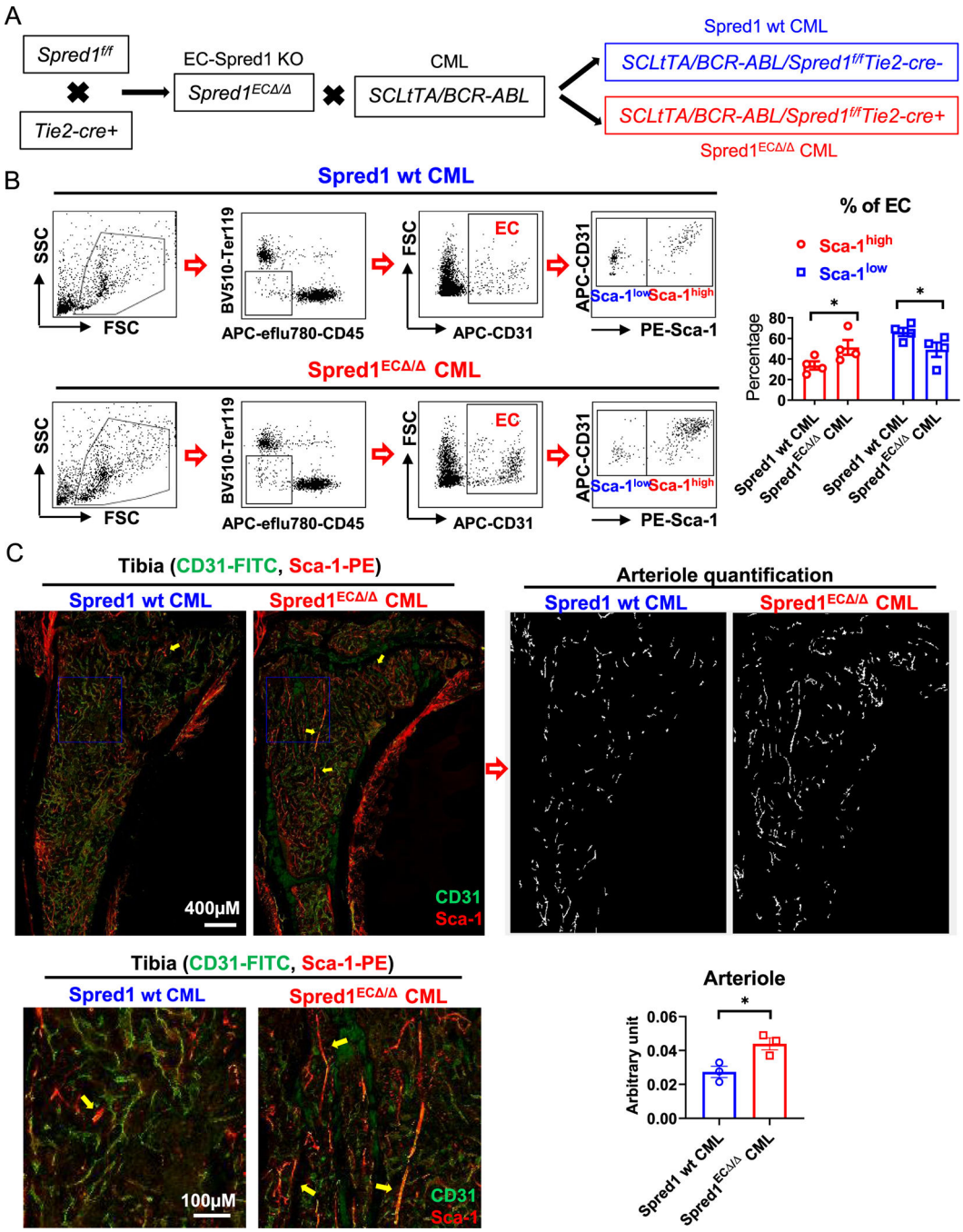

Figure 5. SPRED1 KO in ECs increases arterioles in the BM niche.

A Schematic design of the mouse crossings. *Spred1*$^{f/f}$ (B6-Ly5.2) mouse was crossed with Tie2-Cre+ (B6-Ly5.2; Jax lab, #8863) mouse to generate Spred1$^{f/f}$Tie2-Cre+ (Spred1 KO in ECs, hereafter called Spred1$^{EC\Delta/\Delta}$) mice. Spred1$^{f/f}$Tie2-Cre+ mice were then bred with SCLtTA/BCR–ABL mice to obtain SCLtTA/BCR-ABL/ Spred1$^{f/f}$Tie2-Cre+ (i.e., Spred1$^{EC\Delta/\Delta}$SCLtTA/BCR-ABL, or Spred1$^{EC\Delta/\Delta}$ CML, or EC-Spred1 KO CML) and Cre- (i.e., Spred1 wt SCLtTA/BCR-ABL, or Spred1 wt CML) mice. **B** Representative plots (left) and aggregate results (right) of BM EC Sca-1^{high} and Sca-1^{low} subfractions from Spred1

wt SCLtTA/BCR-ABL and Spred1$^{EC\Delta/\Delta}$SCLtTA/BCR-ABL mice after four weeks of BCR-ABL induction by tet withdrawal, analyzed by flow cytometry (n=4 mice per group). **C** CD31 (FITC) and Sca-1 (PE) immunofluorescence (IF) staining (left, top, tibia; left, bottom, enlarged representative region) and quantification (right, top, arbitrary units representing arterioles; right, bottom, aggregate results of arbitrary units from three representative regions) of CD31^{+}Sca-1^{high} EC-lined vessels (i.e., arterioles, indicated by yellow arrows, see supplementary methods for the details how the arterioles were quantified using arbitrary units) in the tibias from Spred1 wt CML and EC-Spred1 KO CML mice (n=3 mice per group). Results shown represent mean ± SEM. Significance values: *, $p<0.05$.

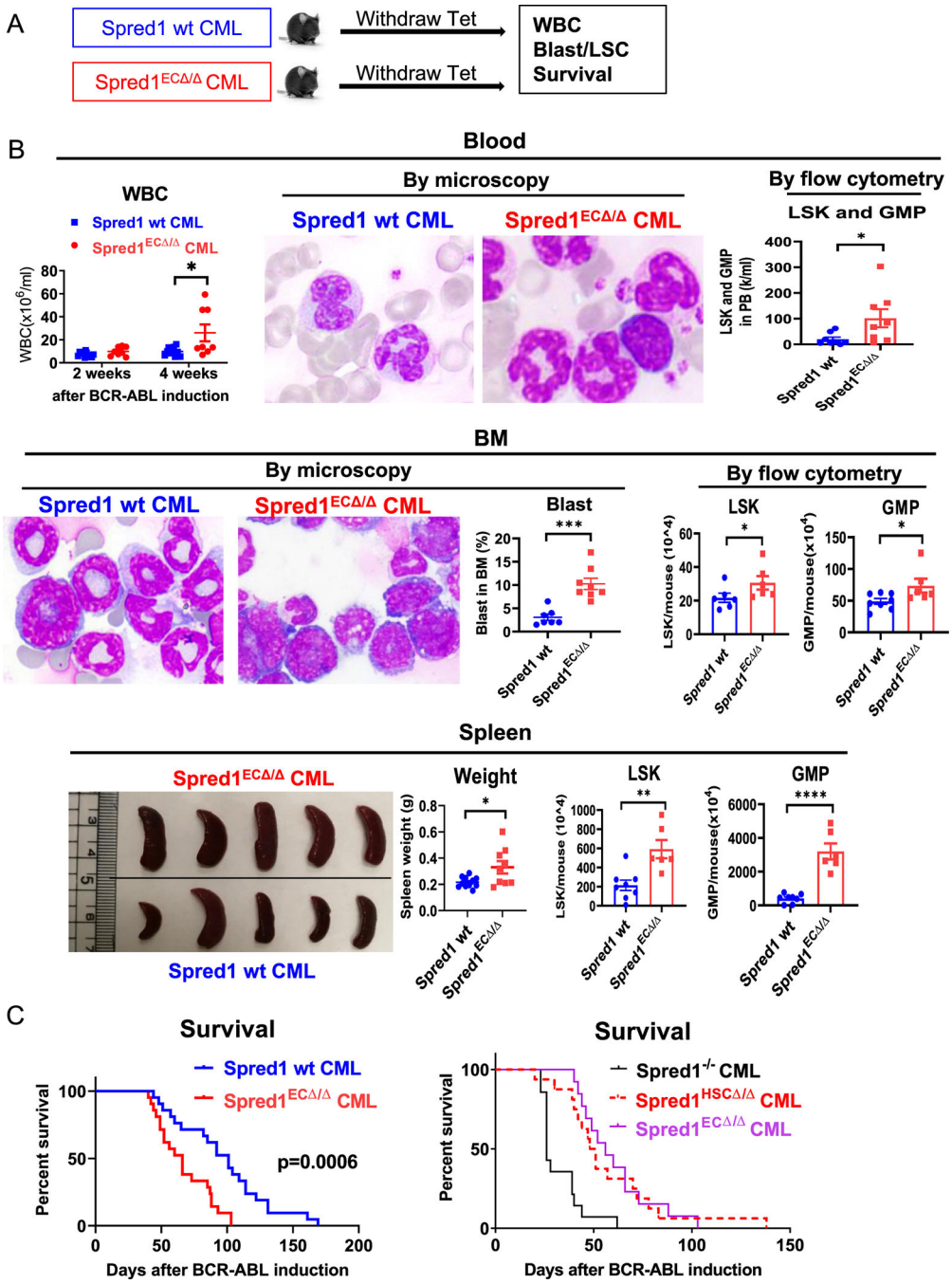

Figure 6. *Spred1* loss in the BM vascular niche independently contributes to CML transformation.

A Schematic design of the experiments. After BCR-ABL induction by tetracycline withdrawal, Spred1 wt SCLtTA/BCR-ABL and Spred1$^{EC\Delta/\Delta}$SCLtTA/BCR-ABL mice were monitored for WBC counts, leukemic blasts and survival. **B** WBC counts, blood and BM leukemic blasts by microscopy and LSK and GMP numbers by flow cytometry, spleen size and weight and LSK and GMP numbers by flow cytometry, in Spred1 wt SCLtTA/BCR-ABL and Spred1$^{EC\Delta/\Delta}$SCLtTA/BCR-ABL mice measured at four weeks

after BCR-ABL induction (n=8 mice per group). **C** Survival of Spred1 wt SCLtTA/BCR-ABL and Spred1$^{EC\Delta/\Delta}$SCLtTA/BCR-ABL mice after BCR-ABL induction (n=13 mice per group, left) and survival of Spred1$^{-/-}$SCLtTA/BCR-ABL (global KO, n=14 mice), Spred1$^{HSC\Delta/\Delta}$SCLtTA/BCR-ABL (HSC KO, n=16 mice) and Spred1$^{EC\Delta/\Delta}$SCLtTA/BCR-ABL (EC KO, n=13 mice) mice after BCR-ABL induction (right). Results shown represent mean ± SEM. Significance values: *, $p<0.05$; **, $p<0.01$; ***, $p<0.001$; ****, $p<0.0001$.

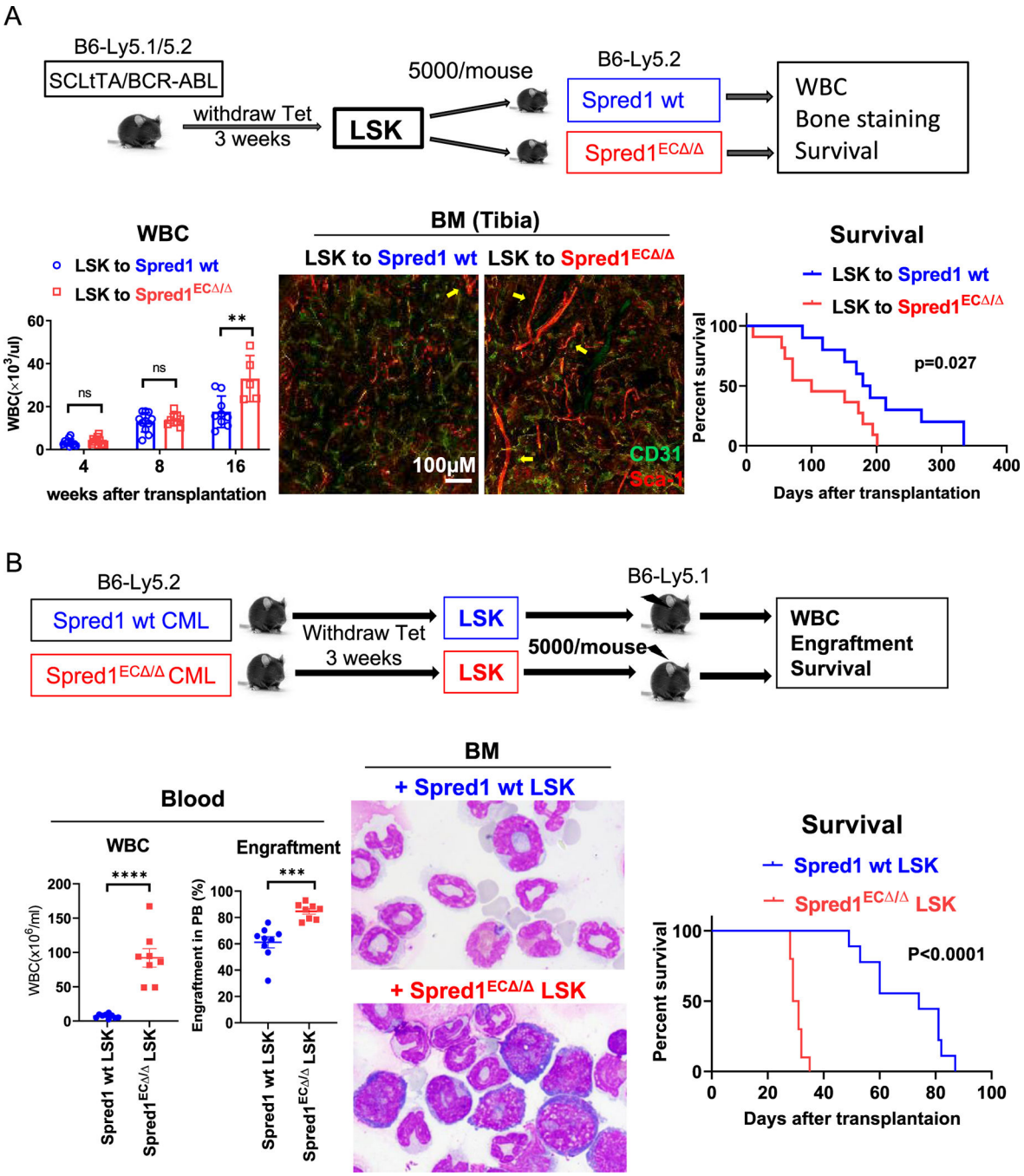

Figure 7. *Spred1* loss in the BM vascular niche independently contributes to CML transformation.

A Schematic design and results of the experiments. LSKs (5000 cells/mouse) from SCLtTA/BCR-ABL CML mice (B6-Ly5.1/5.2, BCR-ABL was induced for three weeks by tet withdrawal) were selected and transplanted into congenic Spred1 wt (B6-Ly5.2, n=14) and Spred1$^{EC\Delta/\Delta}$ (B6-Ly5.2, n=10) recipient mice respectively (top). WBC counts, CD31 (FITC) and Sca-1 (PE) IF staining of CD31^{+}Sca-1^{high} EC-lined vessels (i.e., arterioles, indicated by yellow arrows) in the tibias, and survival (bottom) of the Spred1 wt (n=14)

and Spred1$^{EC\Delta/\Delta}$ (n=10) recipient mice receiving CML LSKs. **B** Schematic design and results of the experiments. LSKs (5000 cells/mouse) from Spred1 wt SCLtTA/BCR-ABL and Spred1$^{EC\Delta/\Delta}$SCLtTA/BCR-ABL mice (both are B6-Ly5.2, BCR-ABL was induced for three weeks by tet withdrawal) were transplanted into congenic normal wt recipient mice (B6-Ly5.1, n=10 mice per group) (top). WBC counts and CML cell engraftment rate in PB by flow cytometry, leukemia blasts in BM by microscopy, and survival of recipient mice (n=10 mice per group) transplanted with LSKs from Spred1 wt CML or Spred1$^{EC\Delta/\Delta}$ CML mice (bottom). Results shown represent mean ± SEM. Significance values: **, $p<0.01$; ***, $p<0.001$; ****, $p<0.0001$; ns, not significant.

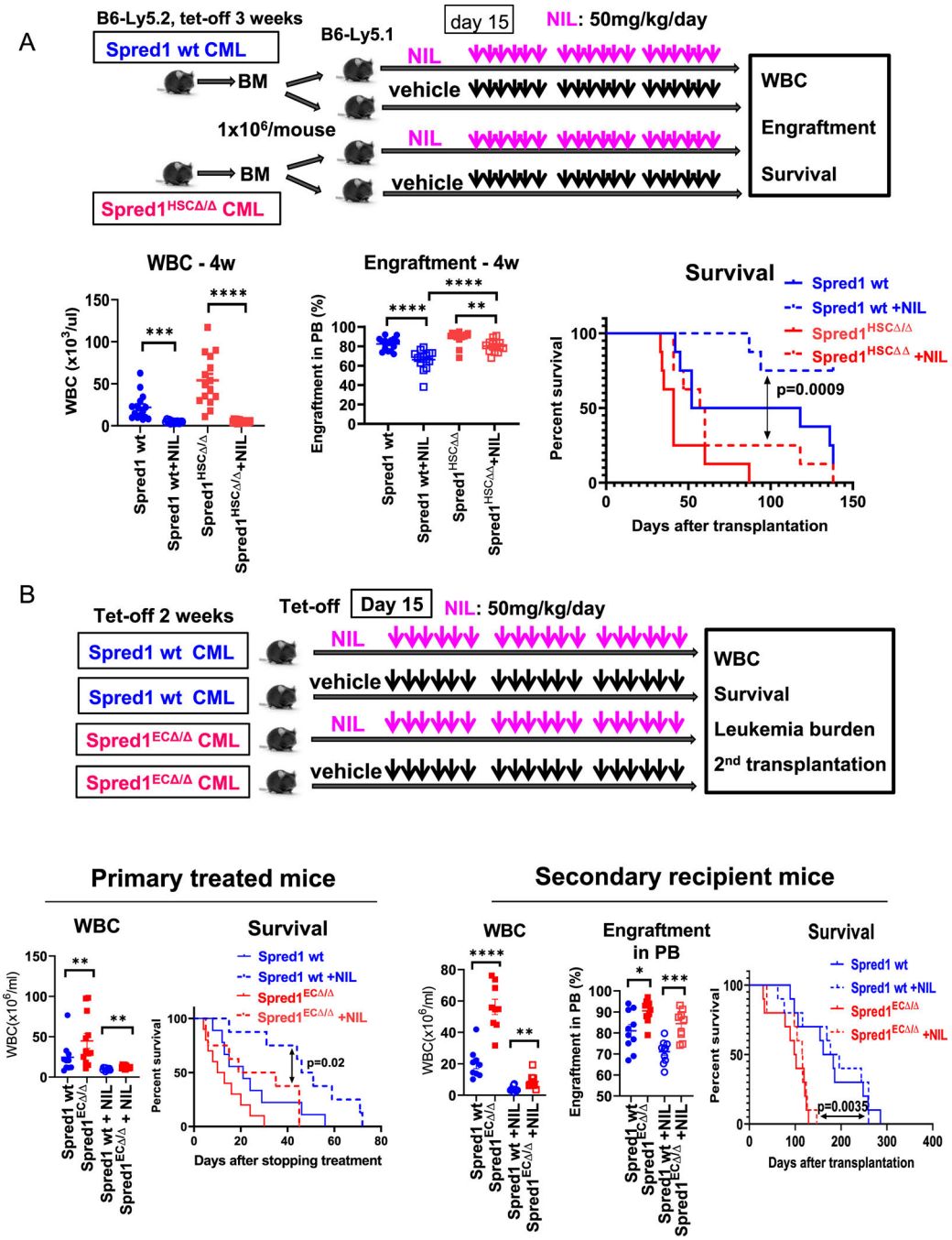

Figure 8. Spred1 depletion promotes TKI resistance in CML.

A Schematic design and results of the experiments. BM cells (1×10^6/mouse) from Spred1 wt SCLtTA/BCR-ABL and Spred1$^{HSC\Delta/\Delta}$SCLtTA/BCR-ABL leukemic mice (B6-Ly5.2, BCR-ABL was induced for three weeks by tet withdrawal) were transplanted into congenic normal wt mice (B6-Ly5.1, n=20 mice per group). Two weeks after transplantation, these mice were divided into four groups and treated with vehicle or nilotinib (NIL, 50mg/kg, oral gavage, daily) for three weeks (wt+vehicle, wt+NIL, HSC KO+vehicle, HSC KO+NIL; top). WBC counts and CML cell engraftment rates in PB measured at four weeks after

transplantation by flow cytometry, and survival of the four groups of mice were shown (bottom). **B** Schematic design and results of the experiments. After two weeks of BCR-ABL induction by tet withdrawal, Spred1 wt SCLtTA/BCR-ABL and Spred1$^{EC\Delta/\Delta}$SCLtTA/BCR-ABL mice (B6-Ly5.2, n=8 mice per group) were treated with NIL (50mg/kg, oral gavage, daily) or vehicle for three weeks. BM cells (1×10^6/mouse) from the treated primary mice were pooled and transplanted into secondary recipient mice (B6-Ly5.1, n=10 mice per group). WBC counts and survival of primary treated mice (bottom, left), and WBC counts, CML cell engraftment rates in PB, and survival of secondary recipient mice (bottom, right) were shown. Results shown represent mean ± SEM. Significance values: *, $p<0.05$; **, $p<0.01$; ***, $p<0.001$; ****, $p<0.0001$.